iScience, Volume *24*

Supplemental information

Rad52 SUMOylation functions as a molecular switch that determines a balance between the Rad51- and Rad59-dependent survivors

Ferose Charifi, Dmitri Churikov, Nadine Eckert-Boulet, Christopher Minguet, Frédéric Jourquin, Julien Hardy, Michael Lisby, Marie-Noëlle Simon, and Vincent Géli

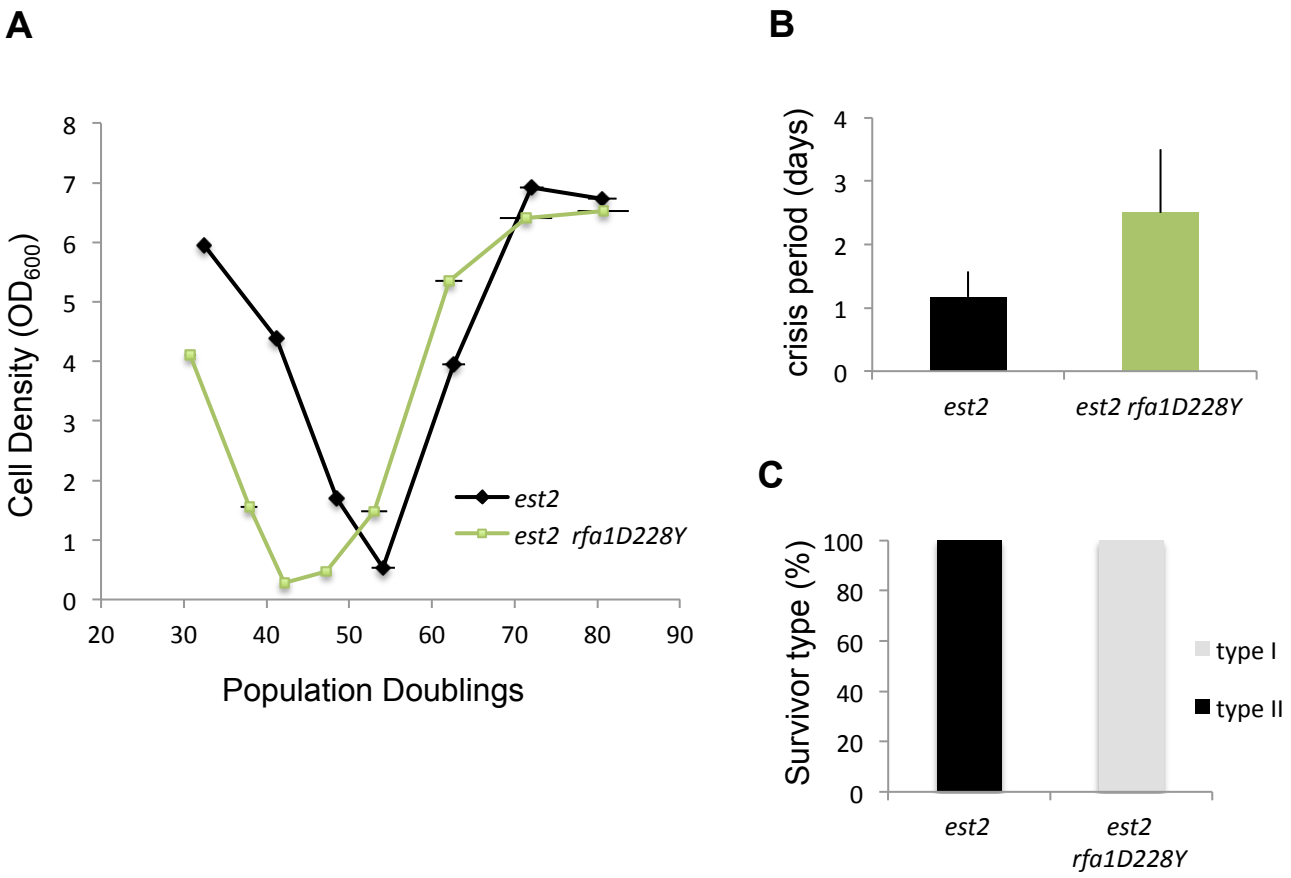

Figure S1. *rfa1-DD228Y* impairs type II recombination (related to Figure 1). (**A**) Mean senescence profiles of *est2Δ* (n=6) and *est2Δ rfa1D228Y* (n=4) clones. Bars are SD. (**B**) The crisis period is determined as the number of days the cell population stays arrested for each individual clones analyzed. Crisis period average calculated for each mutant is represented. Bars are SD (**C**). Relative frequencies of the telomerase-independent survivor types formed by the clones analyzed in (A).

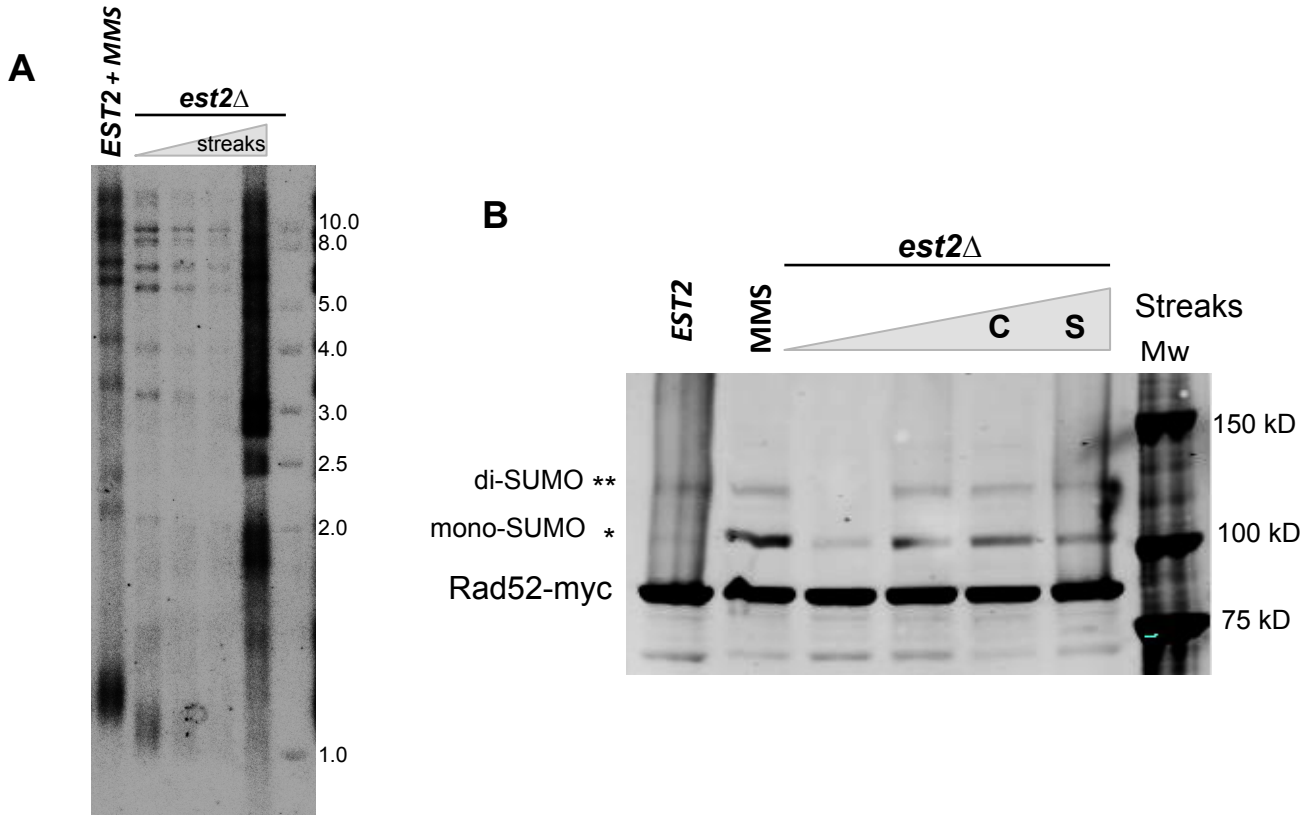

Figure S2. Rad52 is SUMOylated upon telomere erosion (Related to Figure 2). An *est2Δ RAD52-MYC* haploid strain was obtained by sporulating a heterozygous *EST2*/*est2Δ RAD52*/*RAD52-MYC* diploid strain. The *est2Δ RAD52-MYC* haploid was serially streaked 4 times on YPD plates. After each restreak, cells were collected for DNA extraction and whole cell protein extracts. (A) Telomere length was analyzed after *XhoI* DNA digestion by southern blot using a TG_{1-3} probe. (B) At each restreak, cell protein extracts were analyzed by Western-blot using an anti-MYC antibody (9E10). SUMOylated forms of Rad52 are indicated. Extracts from *EST2* cells treated or not with MMS are shown as controls. Crisis (C), Survivors (S).

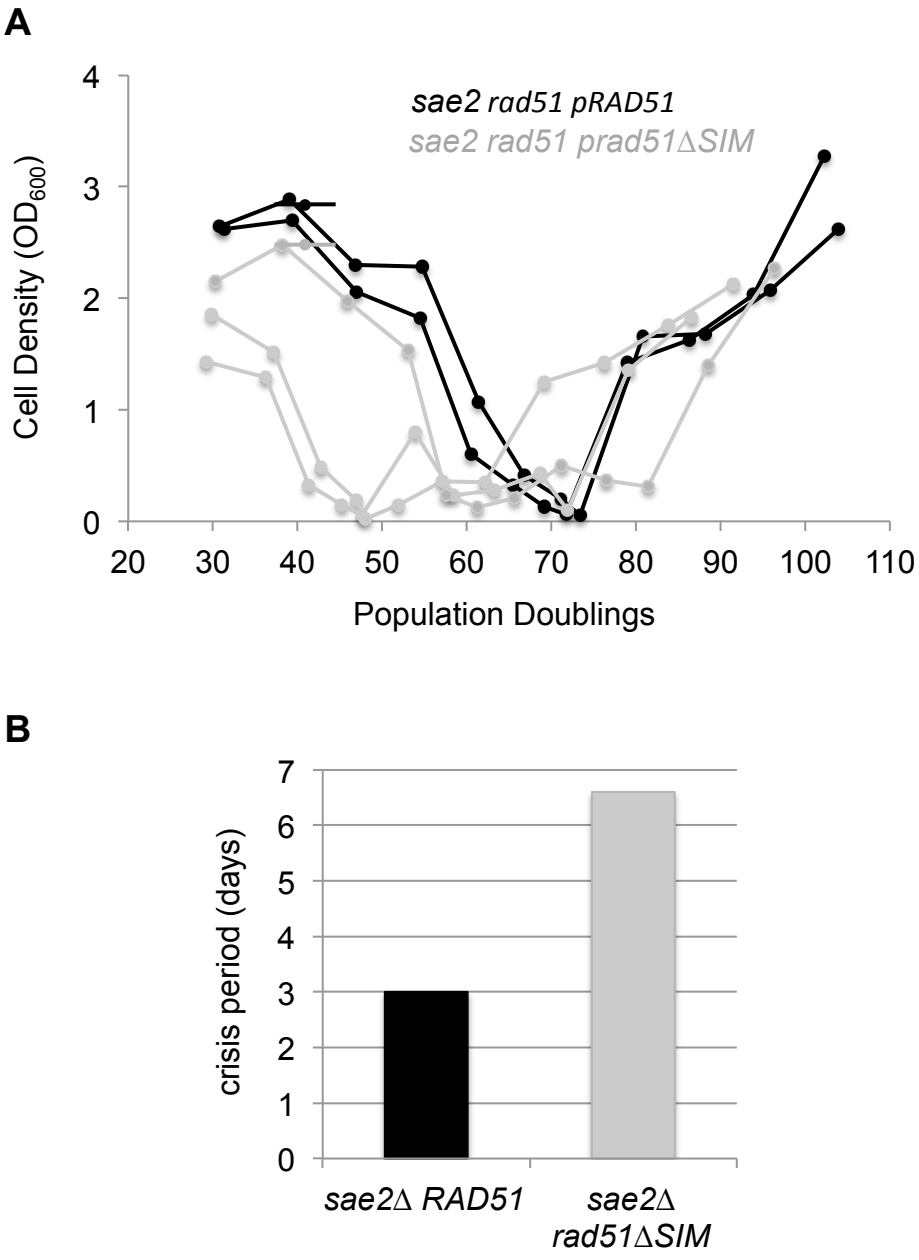

Figure S3. Deleting the SIM domains of Rad51 affects type I recombination (Related to Figure 3). **(A)** Replicative senescence profiles of *est2Δ rad51Δ sae2Δ* cells expressing either WT *RAD51* or *rad51ΔSIM* from a centromeric vector. Senescence was monitored as described above except that the liquid cultures were performed in SC-LEU to maintain the vector. Deleting the SIM domains of Rad51 delays the appearance of survivors**. (B)** Mean time spent in crisis for the clones in (A).

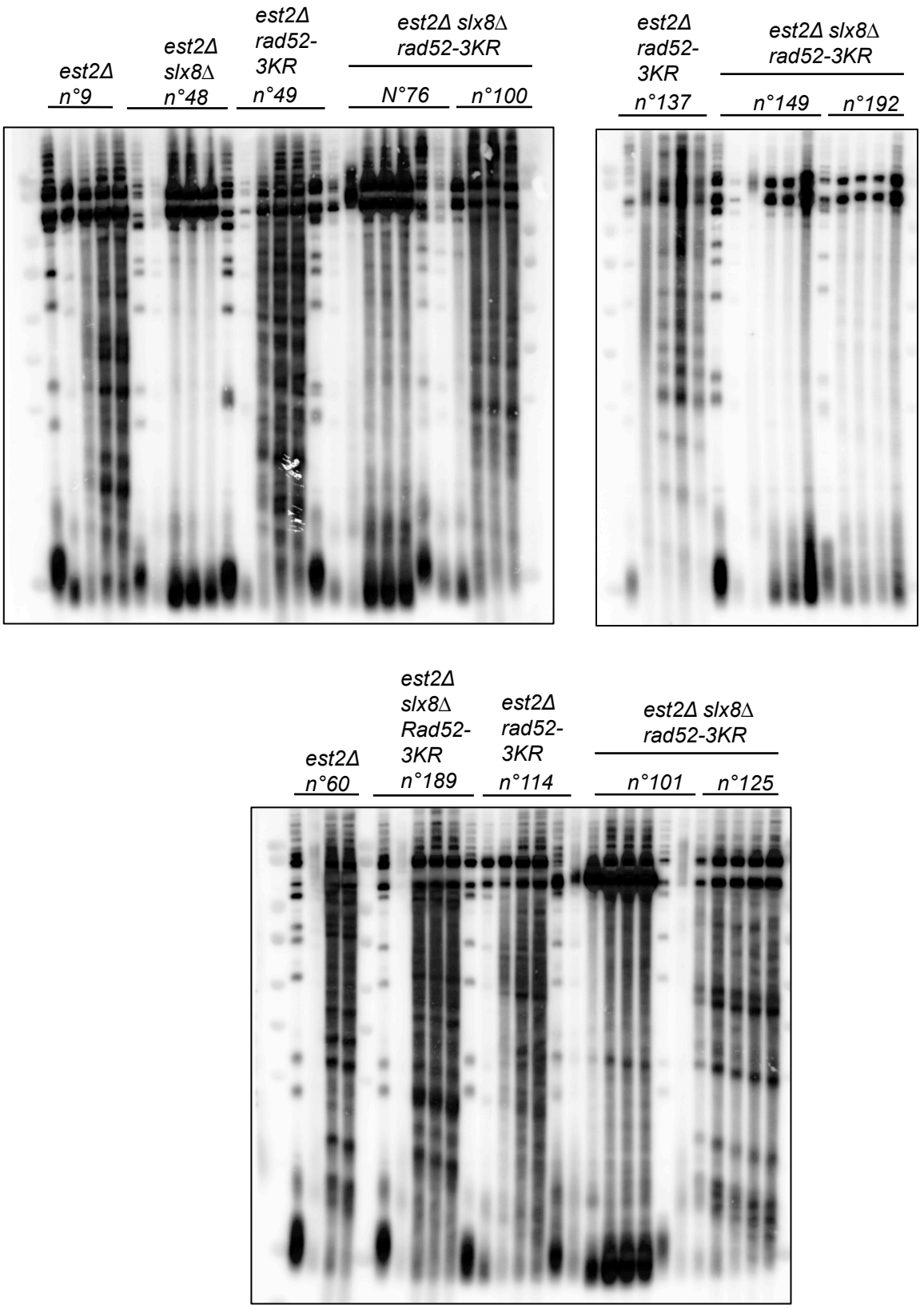

Figure S4. Representative teloblots (related to Figure 4).

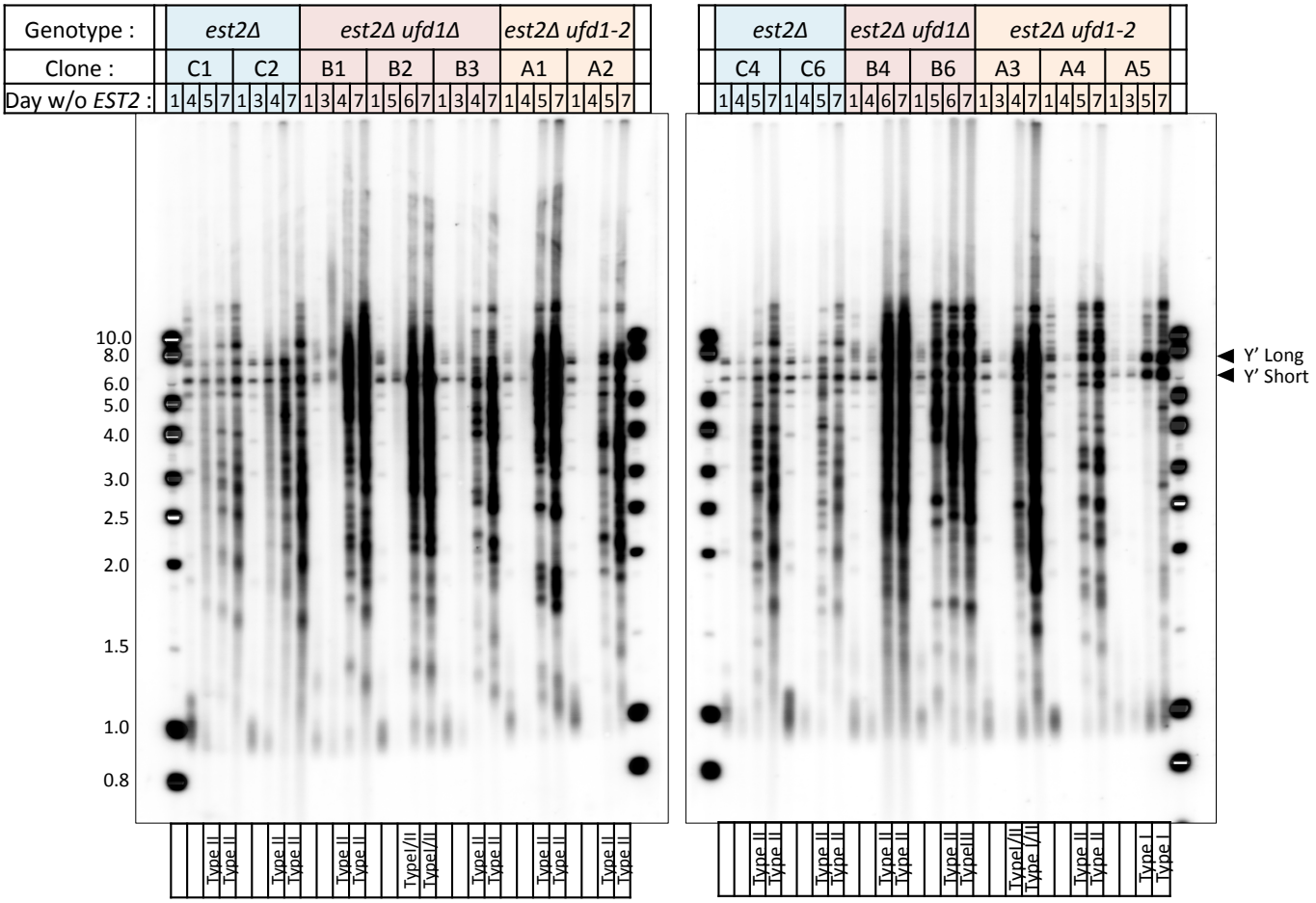

Figure S5. Representative teloblots (related to Figure 5).

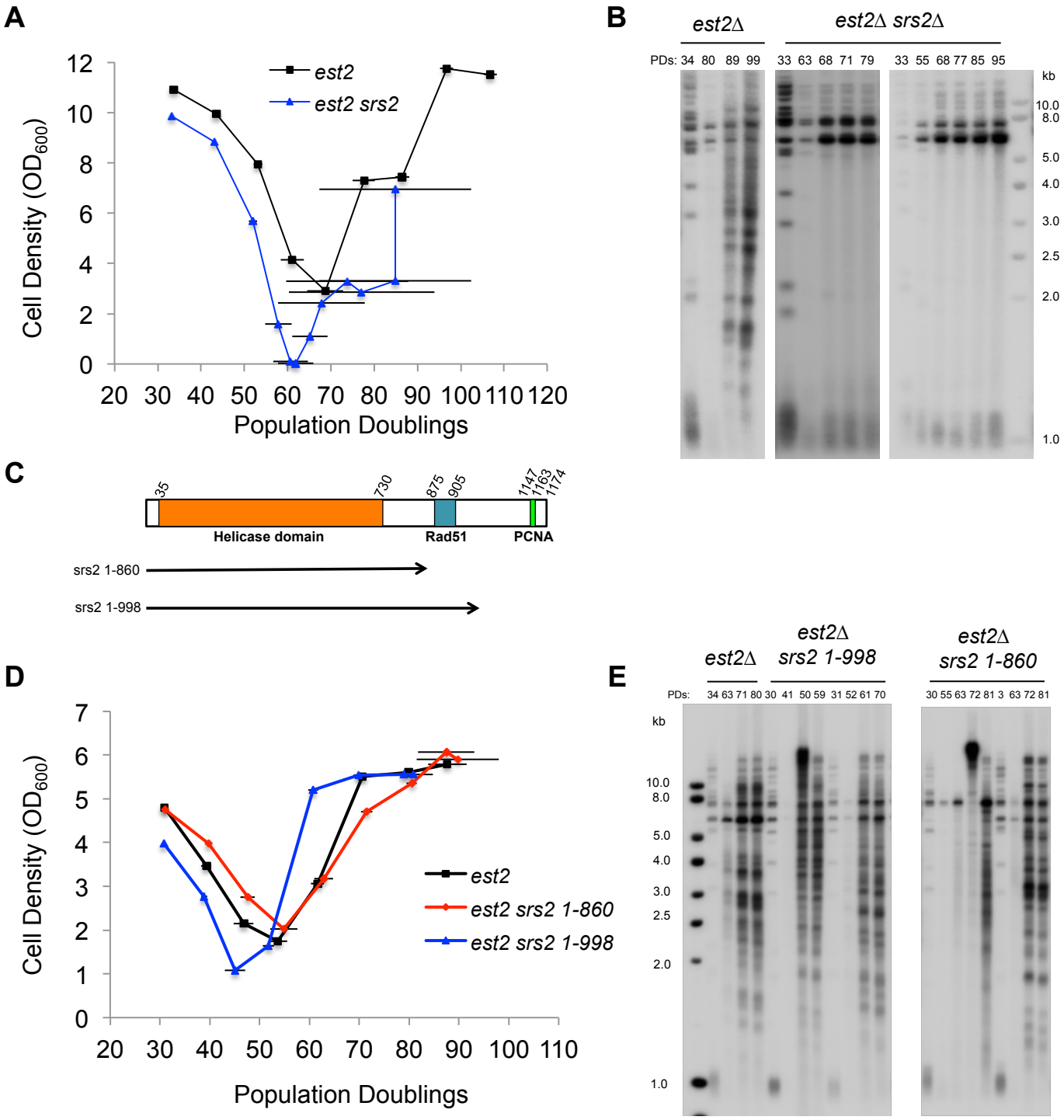

Figure S6. The helicase/antirecombinase Srs2 is required for type II recombination (Related to Figures 3 and 5). (A) Mean senescence profiles of *est2Δ* (n=5), *est2Δ srs2Δ* (n=5) clones. Bars represent SD. (**B**) Telomere length and recombination were analyzed by TG_{1-3} probed Southern blot of *XhoI*-digested DNA prepared from samples of the replicative senescence. The result for two representative clones is shown (5 clones analyzed). (**C**) Schematic representation of the domain organization of Srs2 and of the mutants used in this study. Only the helicase domain and the domains of interaction with Rad51 and PCNA are shown. (**D**) Mean senescence profiles of *est2Δ* (n=8), *est2Δ srs2 1-860* (n=4) and *est2Δ srs2 1-998* (n=10) clones. Bars represent SD. (E) Southern blot of *XhoI*-digested DNA prepared from samples of the replicative senescence. The result for two representative clones is shown for each genotypes.

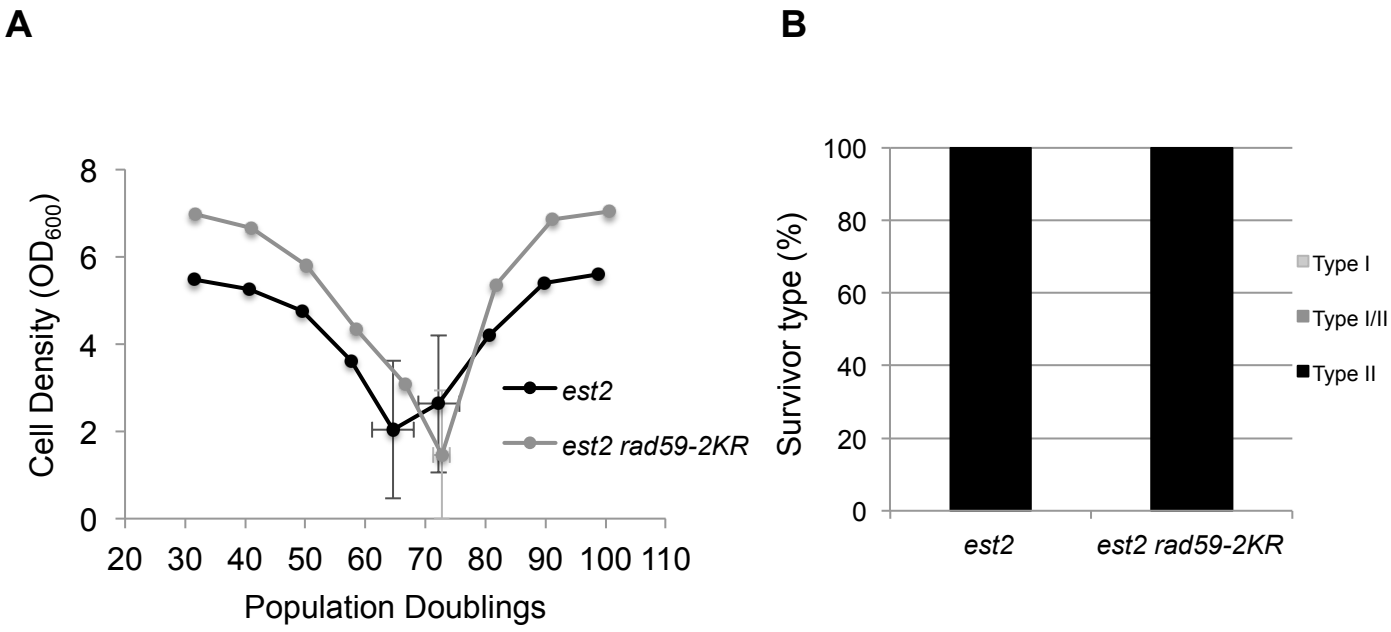

Figure S7. Abolishing Rad59 SUMOylation does not affect NPC type II recombination (Related to Figure 6).

(**A**) Replicative senescence of *est2Δ* and *est2Δ rad59-2KR (n=7)*. (**B**) Relative frequencies of the telomerase-independent survivor types for the *est2Δ* and *est2Δ rad59-2KR*.

Supplementary Table 1: Strains used in this study (related to figures 1 to 7).

Strain	Genotype[1]	Source
ML741-6A	*MAT***a** *RAD52-RFP CDC13-YFP nup133::HIS3 est2::KanMX6 rad51*Δ pNEB21 pUN100-protA-NUP133::LEU2	This study
NEB364-74B	*MAT***a** *RAD52-RFP CDC13-YFP nup133::HIS3 est2::KanMX6 rad59::KanMX6* pNEB21 pUN100-protA-NUP133::LEU2	This study
NEB162-37B	*MAT***a** *RAD52-RFP CDC13-YFP nup133::HIS3 est2::KanMX6* pNEB21 pUN100-protA-NUP133::LEU2	Khadaroo et al., 2009
TG01-8D	*MAT***a** *est2::LEU2 pEST2(URA3)*	AM Bailis
NEB153-10B	*MAT***a** *est2::kanMX6 pEST2(URA3)*	Hardy et al., 2014
DCY5H2	*MAT***a** *RAD5 rfa1-K133,170,427R rfa2-K199R rfa3-K46R* p3x*HA-SLX5* (*LEU2*) 2μ	This study
MNY1508	*MAT***a***/a EST2/est2 ::LEU2 SLX8/slx8 ::KanMX6 RFA1/ rfa1-K133,170,427R RFA2/rfa2-K199R RFA3/ rfa3-K46R*	This study
NEB142-7C	*MAT***a** *RAD5 rad52-K43,44,253R*	This study
FCY337	*MAT***a***/α EST2/est2 ::LEU2 RAD52/rad52-K*43,44,253R	This study
MNY896	*MATα sae2::TRP1*	Hardy et al., 2014
MNY896 x FCY278	*MAT***a***/α EST2/est2::LEU2 RAD52/rad52- K*43,44,253R *SAE2/sae2::TRP pEST2::URA3*	This study
MNY1016	*rad51::LEU2*	Hardy et al., 2014
MNY1016 x FCY278	*MAT***a***/α EST2/est2 ::LEU2 RAD51/rad51 ::LEU2 RAD52/rad52- K*43,44,253R	This study
ML894-4c	*MAT***a** *rfa1-K133,170,427R rfa2-K199R rfa3-K46R*	This study
DCY-5I1	*MAT***α** *rad52-myc* (*NAT*)	This study
ML236-9B	*MATα rad59::KanMX6*	This study
ML236-9B x FCY278	*MAT***a***/α EST2/est2::LEU2 RAD59/rad59::KanMX6 RAD52/rad52- K*43,44,253R	This study
FJY1	*MAT***a***/α EST2/est2 ::KanMX6 SAE2/sae2 ::TRP1 RAD51/rad51 ::KanMX6 pRAD51(LEU2)*	This study
FJY2	*MAT***a***/α EST2/est2 ::KanMX6 SAE2/sae2 ::TRP1 RAD51/rad51::KanMX6 pRAD51*Δ*SIM(LEU)*	This study
ML912-14A	*MAT***a** *RAD52-RFP CDC13-YFP nup133::HIS3 rfa1-K133,170,427R rfa2-K199R rfa3-K46R est2::KanMX6* pNEB21 pUN100-*protA-NUP133* (*LEU2*)	This study
ML825-1D	*MAT***a** *RAD52-RFP CDC13-YFP nup133::HIS3 est2::KanMX6 rad59-K207,228R* pNEB21 pUN100-*protA-NUP133* (*LEU2*)	This study
	*MAT***a***/a EST2/est2::LEU2 UFD1/ufd1*Δ*C::HPH*	This study

MNY1640	*MAT***a**/*a EST2/est2::LEU2 UFD1/ufd1-2*	This study
MNY1455	*MAT***a**/*a EST2/est2::LEU2 SLX8/slx8::KanMX6 RAD52/rad52- K*43,44,253R	This study
2070-5	*MAT***a**/*α EST2/est2 ::KanMX6 rad59::KanMX6/ rad59-K207,228R*	This study
MNY1460	*MAT***a**/*α EST2/est2::KanMX6 NUP1/nup1-LexA::TRP1 SRS2/ srs2::HIS pEST2::URA3*	This study
2070-5	*srs2 2-860::HPH*	Hannah Klein
MNY1522	*MAT***a**/*α EST2/est2::KanMX6 NUP1/nup1-LexA::TRP SRS2/ srs2 2-860::HPH*	This study
MNY1527	*MAT***a**/*α EST2/est2::LEU2 NUP1/nup1-LexA::TRP1 SRS2/srs2 1-998::KanMX6*	This study
MNY1597	*MAT***a**/*α EST2/est2::KanMX6 NUP1/nup1-LexA::TRP1 RFA1/rfa1-D228Y pEST2::URA3*	This study
MNY1528	*Type II survivors MAT***a**/*α est2::LEU2/est2::LEU2 SRS2/srs2::HIS3*	This study
MNY1542	*Type II survivors MAT***a**/*α est2::LEU2/est2::LEU2 PIF1/pif1::KanMX6*	This study
MNY1548	*Type II survivors MAT***a**/*α est2::LEU2/ est2::LEU2 SLX8/slx8::KanMX6*	This study
MNY1565	*Type II survivors MAT***a**/*α est2::LEU2/ est2::LEU2 RAD51/rad51::KanMX6*	This study
MNY1563	*Type II survivors MAT***a**/*α est2::LEU2/ est2::LEU2 RAD59/rad59::KanMX6*	This study

[1] Yeast strains in this study are derivatives of W303-1A (*MAT***a** *BAR1 LYS2 ade2-1 can1-100 ura3-1 his3-11,15 leu2-3, 112 trp1-1 rad5-535*) (Thomas and Rothstein, 1989).

TRANSPARENT METHODS

Strains and Senescence assays

Strains used in this study are described in Table S1. Liquid senescence assays were performed starting with the haploid spore products of diploids that were heterozygous for EST2 (*EST2*/*est2Δ*) and for the gene(s) of interest. To ensure homogeneous telomere length before sporulation, the diploids were propagated for at least 50 PDs in YPD. The entire colonies outgrowing from haploid spores (estimated 20-30 PDs) were inoculated in liquid YPD medium to estimate the number of PDs, diluted to OD600= 0,1 and grown at 30°C. Every 24 hrs, the cell density was measured (OD_{600}), and a fresh 15 ml of YPD culture was inoculated at an estimated density of 10^5 cells per ml. Multiple clones of each genotype were propagated in this manner until the emergence of survivors. Replicative senescence curves shown in this study correspond to the average of several senescence using independent spores with identical genotype. When indicated, the number of days the cell population stays arrested (crisis period) was determined for each individual spore. Senescence assays on solid medium were initiated as described above, but the cells were propagated by consecutive restreaking on solid YPD plates followed by outgrowth for 2 days at 30°C. The process was repeated until the appearance of survivors. Telomere lengths were analyzed by Southern blotting of *XhoI* cut genomic DNA probed with a telomeric TG_{1-3} probe. Type I and II survivors were determined based on their characteristic terminal restriction fragment pattern (Simon et al., 2021). When both type I and II survivors were detected in the same culture, the type was scored as mixed.

Coimmunoprecipitation

Native protein extracts were prepared in HNT buffer (50 mM HEPES, 200 mM NaCl, 1% Triton X-100) at pH 7.5 by cell disruption with glass beads in a Precellys 24 homogenizer (BertinTechnologies, France). To minimize protein degradation and loss of PTMs, the buffer was supplemented with protease inhibitors: 30 mM N-ethylmaleimide (NEM), 1 mM sodium orthovanadate, and EDTA-free complete cocktail (Roche). For IPs the extracts were rotated top over bottom, first for 2 hr with either anti-HA (3F10) or anti-yRFA antibodies, and then for another 1.5 hr with Dynabeads protein G (Invitrogen Dynal AS, Oslo, Norway) at 4°C. The beads were then subjected to stringent washing (5 times in HNT buffer) to remove non-specific background binding to the beads. The bound proteins were eluted by boiling the beads in the Laemmli sample buffer and subjected to immunoblotting. For the experiment

shown in Fig. 1, the extracts were treated with 100 mg/mL of DNase I (Roche) for 30 min on ice prior to IP.

Live cell imaging of senescing cells and fluorescence microscopy

Live-cell imaging was performed on *est2Δ nup133ΔN* cells expressing Rad52-RFP, Cdc13-YFP and CFP-Nup49 (pNEB21) tagged proteins after loss of the pVL291 vector carrying *EST2* (*URA3*) by restreaking on SC-Trp plates and testing for the loss of pEST2-URA3 by replica-plating onto SC-Ura, (Churikov et al., 2016; Khadaroo et al., 2009). Two-to-four independent Ura^- and $5\text{-}FOA^R$ colonies were used to inoculate 20-ml liquid cultures in SC-Trp-Leu+Ade medium (100 μg/ml adenine). These cultures were grown in the shaker incubator at 25°C and diluted to OD_{600} = 0.3 every day. At the time of each dilution, an aliquot of cells was examined by fluorescence microscopy. Generation time was calculated based on OD_{600} measured over consecutive time intervals. Mutant strains (*rad51Δ, rad59Δ*, *rad59-2KR*) were obtained by sporulation of respective hetorozygous diploids followed by selection of spore clones carrying desired combination of markers. Fluorescence microscopy was performed as described (Eckert-Boulet et al., 2011).

Western Blot and antibodies

Protein extracts for Western blot analysis were prepared from trichloroacetic acid (TCA)-treated yeast cells (Azzam et al., 2004). Proteins were resolved on 10% SDS-PAGE and analyzed by standard Western blotting techniques. Monoclonal antibody against the MYC-epitope (9E10) was used to detect Rad52-Myc. Rabbit polyclonal serum against *S. cerevisiae* RFA (AS07 214) was obtained from Agrisera.

Supplemental references:

Azzam, R., Chen, S.L., Shou, W., Mah, A.S., Alexandru, G., Nasmyth, K., Annan, R.S., Carr, S.A., and Deshaies, R.J. (2004). Phosphorylation by cyclin B-Cdk underlies release of mitotic exit activator Cdc14 from the nucleolus. Science *305*, 516–519.

Churikov, D., Charifi, F., Eckert-Boulet, N., Silva, S., Simon, M.-N., Lisby, M., and Géli, V. (2016). SUMO-Dependent Relocalization of Eroded Telomeres to Nuclear Pore Complexes Controls Telomere Recombination. Cell Rep *15*, 1242–1253.

Eckert-Boulet, N., Rothstein, R., and Lisby, M. (2011). Cell biology of homologous recombination in yeast. Methods Mol Biol *745*, 523–536.

Hardy, J., Churikov, D., Géli, V., and Simon, M.-N. (2014). Sgs1 and Sae2 promote telomere replication by limiting accumulation of ssDNA. Nat Commun *5*, 5004.

Khadaroo, B., Teixeira, M.T., Luciano, P., Eckert-Boulet, N., Germann, S.M., Simon, M.N., Gallina, I., Abdallah, P., Gilson, E., Géli, V., et al. (2009). The DNA damage response at eroded telomeres and tethering to the nuclear pore complex. Nat Cell Biol *11*, 980–987.

Simon, M.N., Churikov, D. and Geli, V. (2021) Analysis of recombination at yeast telomeres. Methods Mol Biol *2153*, 395-402.

Thomas, B.J. and Rothstein, R. (1989) The genetic control of direct-repeat recombination in *Saccharomyces*: the effect of rad52 and rad1 on mitotic recombination at GAL10, a transcriptionally regulated gene . Genetics *123*, 725-738.